

The Mira star S Ori: SiO maser shells related to the stellar photosphere, the molecular layers, and the dust shell at three epochs

M. Wittkowski¹, D. A. Boboltz², K. Ohnaka³, T. Driebe³
and M. Scholz^{4,5}

¹European Southern Observatory, Garching, Germany
email:mwittkow@eso.org

²United States Naval Observatory, Washington, DC, USA
email:dboboltz@usno.navy.mil

³Max-Planck-Institut für Radioastronomie, Bonn, Germany

⁴Institut für Theoretische Astrophysik, Heidelberg, Germany

⁵Institute of Astronomy, University of Sydney, Australia

Abstract. We present recent results from our project of concurrent radio and infrared interferometry of oxygen-rich Mira stars. Our pilot study on the Mira variable S Ori included coordinated VLBA mapping of the $v=1$, $J=1-0$ 43.1 GHz and $v=2$, $J=1-0$ 42.8 GHz SiO maser radiation at one epoch and concurrent near-infrared K -band interferometry to constrain the stellar photospheric diameter. We recently obtained new maps of these SiO maser transitions toward S Ori at three additional epochs with the VLBA and concurrent mid-infrared interferometric data with VLTI/MIDI. The MIDI data are analyzed using recent self-excited dynamic model atmospheres including molecular shells close to continuum-forming layers, which we complement by a radiative transfer model of the dust shell. The modelling of our MIDI data results in phase-dependent continuum photospheric angular diameters. The dust shell can best be modelled with Al_2O_3 grains alone. We find that the mean SiO maser ring radii lie between about 1.9 and 2.4 stellar continuum radii. The maser spots mark the region of the molecular atmospheric layers shortly outward of the steepest decrease of the mid-infrared model intensity profile. Our results suggest that the SiO maser shells are co-located with the Al_2O_3 dust shell near minimum visual phase. Their velocity structure indicates a radial gas expansion. Preliminary results from a study of the Mira star GX Mon suggest a similar picture.

Keywords. masers, radiative transfer, techniques: high angular resolution, techniques: interferometric, stars: AGB and post-AGB, stars: atmospheres, circumstellar matter, stars: fundamental parameters, stars: individual (S Ori, GX Mon), stars: mass loss

1. Introduction

Interferometric observations providing a high spatial resolution are best suited to provide further observational constraints on the regions close to the surface where stellar pulsation and dust formation take place and where the mass-loss is initiated. Hereby, interferometry at different wavelength regions is needed to probe different regions: Near-infrared interferometry is most sensitive to the continuum photosphere and to warm molecular layers lying above the photosphere. Mid-infrared interferometry is most sensitive to the molecular layers lying above the photosphere, which cause the mid-infrared diameter to be significantly larger than the near-infrared diameter, and to the dust shell. Complementary information regarding the circumstellar environment can be obtained by observing the maser radiation that some of the molecules emit. The structure and

dynamics of the CSE of Mira variables and other evolved stars can be investigated by mapping SiO maser emission at typically about 2 stellar radii toward these stars using very long baseline interferometry (VLBI) at radio wavelengths.

We have established a program of concurrent infrared interferometry using the VLTI and radio interferometry using the VLBA. The former aims at constraining the photospheric radius, the characteristics of atmospheric molecular layers, and parameters of the dust shell. The latter aims at concurrently mapping the SiO maser emission. Our final goal is a better understanding of the mass-loss process and its connection to stellar pulsation. Our pilot study in Boboltz & Wittkowski (2005) on the Mira variable *S Ori* included coordinated near-infrared *K*-band interferometry to constrain the stellar photospheric diameter and VLBA mapping of the SiO maser radiation toward this source. We have now obtained the first multi-epoch study that includes concurrent radio and mid-infrared interferometry of an oxygen-rich Mira star (Wittkowski *et al.* (2007)), the main results of which we outline in the following sections.

2. Relating the maser shell radius to the photospheric radius

Two basic problems arise when attempting to relate the maser shell radius to the photospheric stellar radius.

Firstly, observational results regarding the detailed relationships between the stellar photosphere and the SiO maser ring often suffer from uncertainties inherent in comparing observations of variable stars widely separated in time and stellar phase as discussed in Boboltz & Wittkowski (2005). We overcome this limitation by obtaining concurrent VLTI and VLBA observations. In our recent study, each combined VLTI/VLBA epoch has a width of less than 4% of the stellar variability period.

Secondly, a further uncertainty in comparing photospheric radii to the extensions of the maser shells arises from the complication that near- and mid-infrared intensity profiles of finite bandwidth include a blend of intensities from continuum-forming layers and overlying molecular layers. This effect has often resulted in over-estimated continuum photospheric diameter values. An overestimated photospheric diameter would result in biased relative distances of the dust shell and the maser ring from the stellar surface even if obtained at the same stellar phase and cycle. We employ a detailed comparison of our observations to dynamic model atmospheres to relate the observable quantities to a meaningful continuum photospheric radius and thus to overcome this limitation.

3. Modeling the molecular atmosphere and the dust shell

Mid-infrared photometric and interferometric data of Mira stars are in general sensitive to details of the structure of the stellar atmosphere in which molecular layers of various geometrical and optical characteristics lie above the continuum-forming photosphere, as well as to the surrounding dust shell. We use the P and M model atmosphere series discussed in Ireland *et al.* (2004a), Ireland *et al.* (2004b) to describe the stellar atmosphere including the continuum photosphere and overlying molecular layers, and add an ad-hoc radiative transfer model of the dust shell. The P and M model series are complete self-excited dynamic model atmosphere of Mira stars. We use the Monte Carlo radiative transfer code `mcsim_mpi` by Ohnaka *et al.* (2006) for the radiative transfer model of the dust shell and use the SED of the dust-free atmosphere model as central source. Lorenz-Martins & Pompeia (2000) have investigated the envelopes of 31 oxygen-rich AGB stars using the IRAS LRS spectra. They classify the objects into three groups, whose IRAS LRS spectra can be modeled using either silicate grains, Al_2O_3 grains, or a mix thereof.

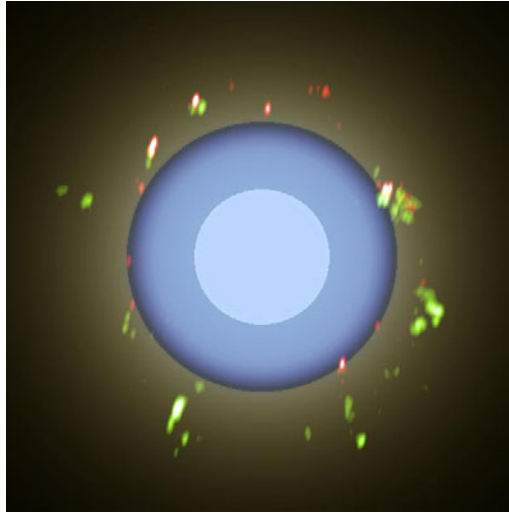


Figure 1. The (red) $v = 2, J = 1 - 0$ (42.8 GHz) and (green) $v = 1, J = 1 - 0$ (43.1 GHz) maser images overlaid onto pseudo-color representations of the infrared intensity for the example of our second epoch from Wittkowski *et al.* (2007). The continuum photosphere is marked by the light blue color. The darker blue shades represent the model intensity profile of the molecular atmosphere seen at mid-infrared wavelengths. The green shades represent the location of the Al_2O_3 dust shell.

We follow their results for the details of the two grain species. Our overall model is thus defined with this set of five independent parameters: (1) choice of the dust-free M model, (2) optical depth of Al_2O_3 , (3) optical depth of silicate (4) inner dust shell boundary (5) dust shell density gradient. We use the well-defined continuum photospheric radius at a wavelength of $1.04 \mu\text{m}$ of the respective dust-free M model to characterize the photospheric radius.

4. VLBA and VLTI measurements

We observed the $v = 1, J = 1 - 0$ (43.1 GHz) and $v = 2, J = 1 - 0$ (42.8 GHz) SiO maser emission associated with S Ori using the 10 stations of the VLBA in January, February, and November 2005. The first two epochs occurred near stellar minimum and were spaced 42 days apart or approximately 10% of the stellar period. The third epoch occurred roughly 9 months later just after maximum on the next stellar cycle. Fig. 1 shows the total intensity images of the two maser transitions for the example of the second epoch compared to the model of our mid-infrared VLTI/MIDI data (described in the next section). In the velocity structure of the masers (not shown here) there appears to be a velocity gradient at all epochs, with masers toward the blue- and red-shifted ends of the spectrum lying closer to the center of the distribution than masers at intermediate velocities. We interpret this effect by a radial expansion of the maser shell with average velocity of about 10 km/sec.

We concurrently obtained mid-infrared interferometry of S Ori with the instrument MIDI at the ESO VLT Interferometer in December 2004, February/March 2005, and November 2005. For the example of our second epoch, Fig. 2 shows the resulting MIDI flux and the MIDI visibility compared to our best-fitting model. For more details on the observations, we refer to Wittkowski *et al.* (2007).

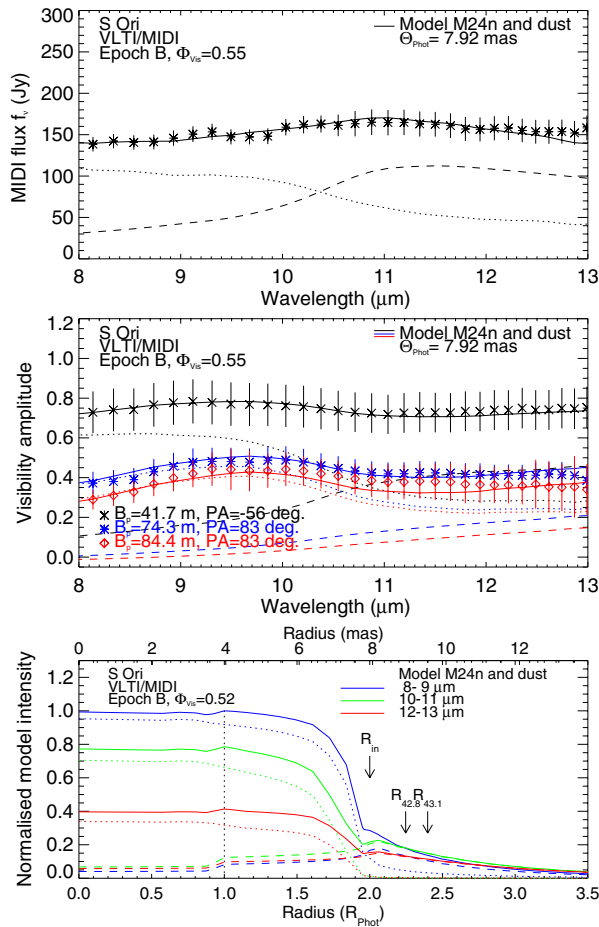


Figure 2. VLTI/MIDI results for the example of our second epoch from Wittkowski *et al.* (2007). Top: MIDI total flux; Middle: MIDI visibility; Bottom: Model intensity profile. The dotted lines denote the contribution from the stellar atmosphere, the dashed line that of the dust shell, and the solid line the overall model.

5. Results

Fig. 3 illustrates the results of our findings for the radial structure of S Ori’s circumstellar environment (CSE) at our near-minimum and post-maximum phases which is widely consistent with the scheme of Reid & Menten (1997). The resulting continuum photospheric angular diameters lie between 7.9 mas and 9.7 mas for the different epochs. The dust shell can well be modelled with Al_2O_3 grains alone and our data shows no indication of silicates, consistent with the modelling of the IRAS LRS spectra by Lorenz-Martins & Pompeia (2000). The inner dust shell angular diameters lie between 1.8 and 2.4 times the continuum photospheric diameters for the different epochs. The 43.1 GHz and 42.8 GHz maser spots show the typical structure of partial to full rings with a clumpy distribution. There is no sign of a globally asymmetric gas distribution. The mean distances of the maser spots from the center of their distribution ranges between 1.9 and 2.4 continuum photospheric radii for the different epochs, with the 42.8 GHz masers lying systematically at closer distances compared to 43.1 GHz masers by about 0.1 continuum photospheric radius. This location of the maser spots is mainly consistent with the modeling by Gray

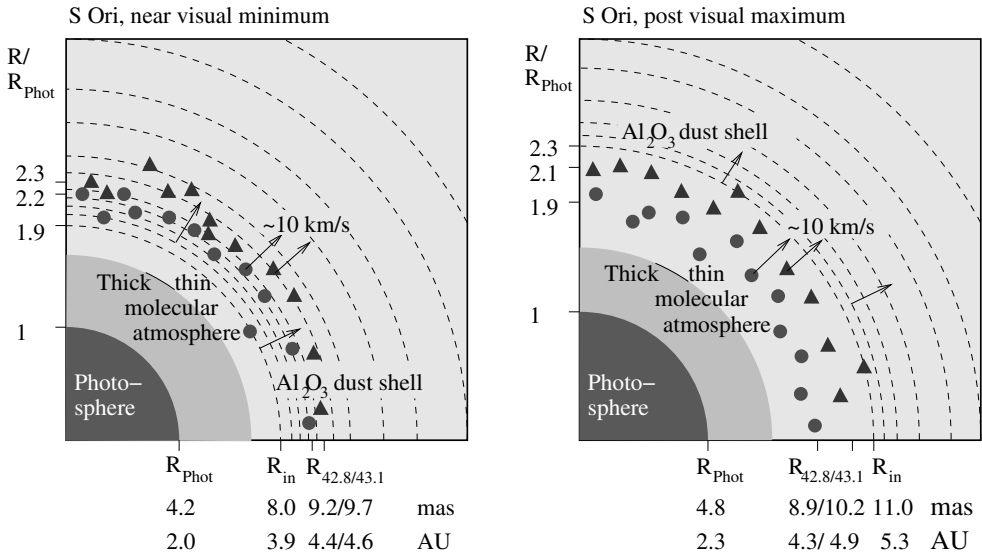


Figure 3. Sketch of the radial structure of S Ori's CSE at (left) near-minimum and (right) post-maximum visual phase as derived in Wittkowski *et al.* (2007). Shown are the locations of (dark gray) the continuum photosphere, (medium dark gray) the at *N*-band optically thick molecular atmosphere, (light gray) the at *N*-band optically thin molecular atmosphere, (dashed arcs) the Al_2O_3 dust shell, and (circles/triangles) the 42.8 GHz and 43.1 GHz maser spots.

& Humphreys (2000) and Humphreys *et al.* (2002), while details of the variability and widths of the maser ring radii may differ from the model predictions. Compared to the molecular atmosphere, the maser shells mark the region of the molecular atmosphere shortly outward of the steepest decrease of the mid-infrared model intensity. Compared to the dust shell, the maser spots are co-located with the inner dust shell near stellar minimum. At our post-maximum phases, the maser spots remain at about the same location, while the dust shell has expanded outward.

Preliminary results from a study of the Mira variable GX Mon using the same technique suggest a similar picture, but where the MIDI data indicates dust shells of corundum *and* silicates with the silicate shell being located farther outward compared to the corundum shell (work in preparation).

References

- Boboltz, D. A. & Wittkowski, M. 2005, *ApJ* 618, 953
 Gray, M. D. & Humphreys, E. M. L. 2000, *New Astron.* 5, 155
 Humphreys, E. M. L., Gray, M. D., Yates, J. A., *et al.* 2002, *A&A*, 386, 256
 Ireland, M. J., Scholz, M., & Wood, P. R. 2004a, *MNRAS* 352, 318
 Ireland, M. J., Scholz, M., Tuthill, P. G., & Wood, P. R. 2004b, *MNRAS* 355, 444
 Lorenz-Martins, S. & Pompeia, L. 2000, *MNRAS* 315, 856
 Ohnaka, K., Driebe, T., Hofmann, K.-H., *et al.* 2006, *A&A* 45, 1015
 Reid, M. J. & Menten, K. M. 1997, *ApJ* 476, 327
 Wittkowski, M., Boboltz, D. A., Ohnaka, K., Driebe, T. & Scholz, M. 2007, *A&A* submitted